JMEPEG (2010) 19:1276–1283
DOI: 10.1007/s11665-010-9633-1

1059-9495/$19.00

Cold Heading of Cylindrical PVC Billets: An Experimental and Theoretical Investigation

L.M. Alves and P.A.F. Martins

(Submitted July 6, 2009; in revised form January 15, 2010)

The design of upset forged metal parts by cold heading is presently well established. Major operating parameters are identified and the typical modes of deformation that may occur during the process are fully characterized. In contrast to metals, there is no research work and no practical design rules in the specialized literature concerning the cold heading of polymer parts. This paper is concerned with the abovementioned lack of knowledge and is a contribution toward the application of cold heading to polymers. The experimental research work makes use of polyvinyl chloride (PVC) and the overall findings are interpreted in the light of an innovative extension of the flow formulation that is capable of modeling cold forming of pressure-sensitive materials under a nonassociated flow rule. Emphasis is placed on the deformation mechanics of cold heading applied to PVC and on the influence of the major operating parameters on the overall formability limits of the process. Results show that cold heading of PVC can be successfully utilized for producing upset forged parts.

Keywords cold heading, experimentation, finite element method, PVC

1. Introduction

Heading can be defined as a bulk forming process accomplished by applying force by a tool to the free end of a stock in the direction of its axis while constraining the other end in a die (Fig. 1). The temperature range for heading runs from cold to hot. Its largest application field is in cold forming of standard metallic fasteners such as screws, bolts and rivets and the manufacture of flanged shafts.

Cold heading represents, nowadays, a very important industrial activity that is expected to evolve and expand in the coming years as a result of continuous innovation and improvement in machine tools and wider variation in the choice of raw materials (Ref 1). New developments and trends in microfabrication are also extending the application of cold heading to the manufacture of parts in the submillimeter range. These facts, together with the continuously growing application of polymers in industry, made authors wonder if the scope of application of cold heading could be extended to include the production of polymer parts.

Polymers are corrosion-resistant with high strength-to-weight ratio. In assembly design, polymers are easier and cheaper to use than metals due to its low elastic modulus. However, despite the potential of cold heading to open new market opportunities and stimulate innovations among polymer products, no applications are currently found in industry because polymer engineering is strongly ingrained in conventional heating-shaping-cooling manufacturing routes.

What is perhaps surprising is the fact that current state-of-the-art within the materials forming research community is not so much different than in industry. In contrast to the investigation on cold heading of metals that finds support in the pioneering analytical studies of the stress field by Lecocq (Ref 2), in the early two-dimensional finite element analysis of the compression of cylinders performed by Shah and Kobayashi (Ref 3), in the establishment of process formability windows relating the reduction in height with the upset ratio by Lange (Ref 4) and in the numerical and experimental analysis of the three-dimensional buckling behavior of tall cylindrical billets performed by Mori et al. (Ref 5), the analysis of cold heading of polymers has, not yet, received attention. In addition to this, published research work in the field of cold forming of polymers is scarce, as can be concluded from the bibliographical reviews published by Mackerle (Ref 6, 7).

Notations	
$F(\sigma_{ij})$	yield function
k	shear yield stress
K	penalty constant
m	friction factor
Q	plastic potential
δ_{ij}	Kronecker delta
$\dot{\varepsilon}_{ij}$	strain rate tensor
$\dot{\varepsilon}_{v}$	volumetric strain rate
$\dot{\bar{\varepsilon}}$	effective strain rate
$\dot{\lambda}$	scalar factor of proportionality
σ_{ij}	stress tensor
σ_{C}	compressive flow stress
σ_{T}	tensile flow stress
$\bar{\sigma}$	effective stress

L.M. Alves and **P.A.F. Martins**, IDMEC, Instituto Superior Tecnico, TULisbon, Av. Rovisco Pais, 1049-001 Lisbon, Portugal. Contact e-mail: pmartins@ist.utl.pt.

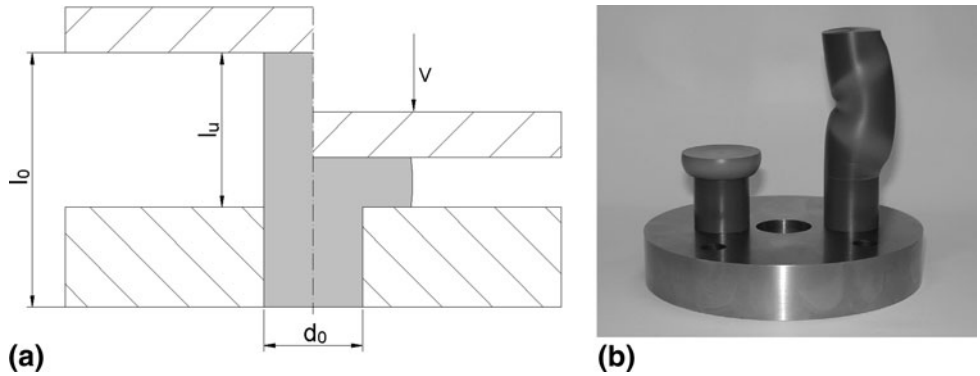

Fig. 1 Cold heading of cylindrical PVC billets. (a) Schematic representation of the process and (b) lower die with successful and nonsuccessful cold headed parts

Table 1 Technical and economical aspects of polymer processing

	Equipment cost	Tooling cost	Production rate	Batch size (number of parts)	Applications
Blow molding	Medium	Medium	Medium	$>10^3$	Hollow thin-walled parts such as bottles, containers and fuel tanks
Compression molding	High	Medium	Medium	$>10^3$	Parts similar to closed-die forgings primarily made from highly filled polymers with a high viscosity
Injection molding	High	High	High	$>10^4$	Complex shapes of various sizes with fine details such as gears, fasteners, housings, switches, and knobs
Transfer molding	High	High	Medium	$>10^3$	More complex parts than those produced by compression molding
Thermoforming	Low	Low	Low	$>10^2$	Parts with shallow or deep cavities made from polymer sheets such as packaging cases
Cold forming	Medium	Low to medium	Medium	$>10^1$	Parts similar to open and close-die forgings in direct competition with compression, injection and transfer molding

This paper was designed in order to provide two contributions to knowledge. The first derives from the application of cold heading to a new class of materials (polymers). The second draws from the identification of a new and fundamental level of understanding about a process and a new class of materials with large potential of utilization in industrial applications.

As a first step toward the objective of extending the scope of application of cold heading to polymers, Table 1 presents a brief overview of the main technical and economical aspects of the conventional polymer processing technologies and forecasts the potential niche market for cold forming applications. In broader terms, this paper is expected to transfer knowledge that will enable readers to address the following three key technical questions; Is the maximum initial height-to-diameter ratio of a polymer billet that prevents failure by buckling smaller or larger than in metals? Is formability exclusively limited by buckling or may, eventually, be influenced by other phenomena such as crazing? Is the influence of geometrical irregularities in the overall deformation of the polymer billets more or less pronounced than in metals?

The paper draws from an innovative extension of the finite element flow formulation, which is capable of modeling cold plastic deformation of polymers under the combined utilization of a pressure-sensitive yield surface and a nonassociated flow rule, to the deformation mechanics of the cold heading of polymers. The influence of material flow and crazing on the occurrence of successful and unsuccessful modes of deformation is comprehensively analysed with the objective of establishing the formability limits of the process and setting-up practical design rules in terms of the major operating parameters. The investigation is supported by means of experimental benchmark tests performed with industrial polyvinyl chloride (PVC) billets under laboratory-controlled conditions. Results confirm that cold heading can be successfully utilized for producing upset parts from cylindrical PVC billets.

2. Theoretical Background

This section provides a general overview of the cold forming of polymers and presents the essentials of the extended finite element flow formulation for pressure-sensitive materials that will be employed in the numerical modeling of cold heading.

2.1 Cold Forming of Polymers

The fundamentals of cold forming of polymers have been comprehensively investigated since the mid-1960s. Whitney and Andrews (Ref 8) proposed a pressure-modified Tresca yield criterion and Sternstein and Ongchin (Ref 9) developed a first version of the pressure-modified von-Mises yield criterion which was later enhanced by Raghava et al. (Ref 10) and

Caddell et al. (Ref 11) in order to explicitly account for the differences between the tensile σ_T and compressive σ_C flow behavior of polymers.

The yield function $F(\sigma_{ij})$ due to Raghava et al. (Ref 10) and Caddell et al. (Ref 11) is expressed as,

$$F(\sigma_{ij}) = \bar{\sigma}^2 - \sigma_C \cdot \sigma_T + (\sigma_C - \sigma_T)\,\sigma_{kk} = 0, \quad \text{(Eq 1)}$$

where $\bar{\sigma}$ is the effective stress and $\sigma_{kk} = \delta_{ij}\,\sigma_{ij}$. The tensile σ_T and compressive σ_C flow stresses are obtained from material characterization (refer to Section 3.1) and in case $\sigma_T = \sigma_C$, the traditional von-Mises criterion (currently utilized in metals) results.

In what concerns incompressibility several researchers have stated, after measuring the volume variation of different polymers, that there is negligible volume variation after yielding. They also concluded that the normality rule, typical of associated plasticity, do not hold in case of pressure-dependent yield surfaces of polymers because it leads to predictions of volume variation at least one order of magnitude larger than observed (Ref 12).

2.2 Extended Finite Element Flow Formulation

Numerical modeling of cold heading was accomplished by employing a modified version of the finite element computer program I-FORM that has been utilized and extensively validated against experimental measurements of metal forming processes since the end of the 1980s (Ref 13). I-FORM performs two- and three-dimensional numerical simulations based on the finite element flow formulation and the modifications performed by the authors allowed extending the approach in order to provide the following innovative functionalities:

(i) Capability of modeling the incompressibility of polymers in the plastic deformation regime.
(ii) Capability of analysing the cold plastic deformation of pressure-sensitive polymers with stress-strain curves exhibiting different strengths in tension σ_T and compression σ_C.
(iii) Capability of locating the initiation sites and the instant of deformation when propagation of crazes is likely to start.

The extended finite element flow formulation considers the polymer as an isotropic plastically deformable body occupying an open bounded domain V with a sufficiently smooth boundary. The boundary consists of several portions; S_u is the part of the boundary S on which the velocity $\bar{u}_i$ is prescribed, while S_t and S_f are the remaining parts on which traction t_i and frictional stress τ_f are applied. The unknown variables are the velocity u_i and the stress field σ_{ij} resulting from the following set of equations,

$$\sigma_{ij,j} = 0 \quad \text{(Eq 2)}$$

$$\dot{\varepsilon}_{ij}(u) = \frac{1}{2}\left(\frac{\partial u_i}{\partial x_j} + \frac{\partial u_j}{\partial x_i}\right) = \frac{1}{2}\,(u_{i,j} + u_{j,i}) \quad \text{(Eq 3)}$$

$$\dot{\varepsilon}_{ij} = \dot{\lambda}\frac{\partial Q(\sigma_{ij})}{\partial \sigma_{ij}} \quad \text{(Eq 4)}$$

The constitutive equation (Eq 4) is built upon a nonassociated flow rule, where $Q = J_2$ is the plastic potential of the conventional von-Mises plasticity and $\dot{\lambda}$ is a positive scalar factor of proportionality, as a result of the incompressibility of polymers in the plastic deformation regime (Ref 14, 15).

In addition, it is expected that the solution for cold forming of polymers should generally meet the following boundary conditions,

$$u_i = \bar{u}_i \quad \text{on } S_u \quad \text{(Eq 5)}$$

$$(u - u_{tool})_i n_i = 0 \quad \text{on } S_f \quad \text{(Eq 6)}$$

$$\sigma_{ij} n_j = t_i \quad \text{on } S_t \quad \text{(Eq 7)}$$

$$\sigma_{ti} = \sigma_{ij}\,n_j - ((\sigma_{kl}\,n_l)\,n_k)\,n_i = \tau_{fi} = -\,|\,\tau_f|\frac{\tilde{u}_i}{|\Delta u_f|} \text{ on } S_f \quad \text{(Eq 8)}$$

where σ_{ti} denotes the tangential component of stress at the contact interface, S_f, between the polymer and tooling and, $|\Delta u_f| = \sqrt{\tilde{u}_i \cdot \tilde{u}_i}$ is the norm of the relative slipping velocity, $\tilde{u}_i = (u - u_{tool})_i$ along S_f (where friction shear stresses τ_{fi} are applied and $|\tau_f|$ is its norm).

Under these circumstances, the variational principle associated with the irreducible extended flow formulation considers the admissible velocity field u_i to be the solution of the problem only if it corresponds to the absolute minimum of the total potential energy rate $\Pi(u_i)$,

$$\Pi\,(u_i) \cong \int_V \left(\int \bar{\sigma}\,d\dot{\bar{\varepsilon}}\right) dV + \frac{K}{2}\int_V \dot{\varepsilon}_v^2 dV - \int_{S_t} t_i u_i\,dS + \int_{S_f}\left(\int_0^{|u_f|} \tau_{fi}\,du_f\right) dS, \quad \text{(Eq 9)}$$

where the flow stress $\bar{\sigma}$ takes into consideration the strength differential effect (that is, the difference between tensile and compressive flow behavior), as required by the yield function proposed by Raghava et al. (Ref 10) and Caddell et al. (Ref 11) for the cold forming of polymers (Ref 1) and K is a large positive constant penalising the volumetric strain rate component, $\dot{\varepsilon}_v$, in order to enforce incompressibility. The norm of the friction shear stress is modeled through the utilization of the law of constant friction $\tau_f = mk$, where m is the friction factor and k is the shear flow stress.

The numerical evaluation of the volume integrals included in Eq 9 is performed by means of a standard discretization procedure based on the utilization of finite elements. In order to ensure the incompressibility requirements of the cold plastic deformation of polymers, both complete and reduced Gauss point integration schemes are utilized. The numerical integration of the friction boundary integral is performed by means of a five Gauss point quadrature. Further details on the finite element discretization of Eq 9 can be found elsewhere (Ref 13).

The accumulation of crazes in some polymers submitted to tensile states of stress below the glass-transition temperature often results in a progressive change of color. I-FORM handles the occurrence of crazing mechanisms by means of the normalized version of the stress-bias criterion (Ref 16),

$$\frac{\sigma_1}{\sigma_0} = \sqrt{1 - R + R^2}, \quad \text{(Eq 10)}$$

where $R = \sigma_2/\sigma_0$, σ_0 is the craze opening stress (refer to Section 3.1), σ_1 is the first principal stress and σ_2 is the second principal stress at craze initiation.

2.3 Modeling Conditions

Finite element computer models of cold heading were set-up in order to reproduce the experimentally observed modes of deformation (Fig. 1). When the material flowed uniformly around its axis of compression and made possible the formation of sound concentric cold headed parts, the analysis was performed by means of either two-dimensional (axisymmetric) or three-dimensional finite element models. Two-dimensional models were based on the discretization of the initial cross section of the billets by means of four-node quadrilateral elements and on the description of the contour of the dies through the utilization of contact-friction linear elements. Three-dimensional models required discretization of the billets by means of eight-node hexahedral elements and definition of tooling by the use of contact-friction spatial linear triangular elements.

In the cases where material flow was nonuniform and buckling was triggered at the early stages of deformation, the simulations were exclusively performed by means of three-dimensional finite element models. In these cases, there was a need to artificially introduce a small irregularity in the upper platen (corresponding to a deviation from flatness below 0.5% in length) in order to stimulate buckling and avoid numerical difficulties. No intermediate remeshing operations were utilized and, therefore, no influence of field variable recovery techniques on the final results needed to be taken into consideration.

The numerical simulations were accomplished through a succession of displacement increments each of one modeling approximately 0.1% of the initial billet length. The convergence of the numerical simulations was stable and the overall CPU time for a typical two dimensional analysis containing roughly 2000 elements was below 2 min on a standard laptop computer. In case of three-dimensional analysis containing approximately 6000 elements, the CPU time ranged from 2 to 4 h as a function of the complexity of the material flow and of the total amount of displacement increments that were necessary to fulfill before reaching the desired level of deformation.

3. Experimental Background

Formability in cold heading is directly related to the unsupported length of the billets (Fig. 1). In case of carbon or alloy steels, the maximum unsupported length l_u is about 2.5 times the diameter d_0 because, beyond this threshold, the billet may buckle (or bend), forcing the material to flow nonuniformly around its axis of compression and preventing the formation of a concentric part. To extend the application of cold heading to polymers and to characterize its formability limits it is important to understand the role played by the material during the process. The cold heading experiments were performed with commercial PVC in the "as-received" condition. Mechanical behavior of PVC and experimental plan are presented below.

3.1 Material Data

The true stress true strain behavior of PVC, shown in Fig. 2, was obtained by means of uniaxial tensile and compression tests. The test specimens were machined from the supplied rods. As seen, the stress-strain curve of PVC is dependent on hydrostatic pressure, giving rise to differences between tensile and compressive flow stress at a given strain. This phenomenon is commonly known as the strength differential effect (SD) and is typical of the cold deformation of PVC.

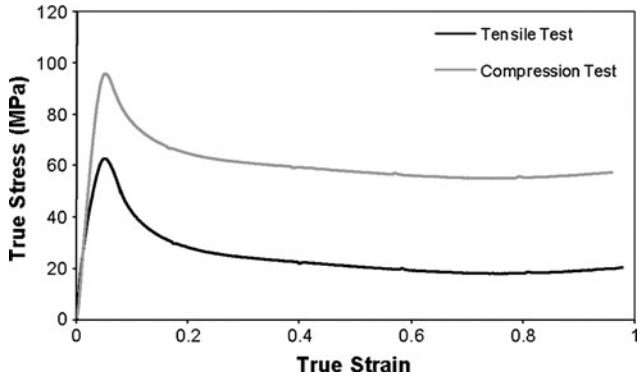

Fig. 2 True stress-strain curves of PVC from tensile and compression tests

Table 2 The plan of experiments

Case	Material	d_0, mm	l_0, mm	l_u, mm	l_u/d_0
1	PVC	22	33	11	0.5
2	PVC	22	38.5	16.5	0.75
3	PVC	22	44	22	1
4	PVC	22	49.5	27.5	1.25
5	PVC	22	55	33	1.5
6	PVC	22	66	44	2
7	PVC	22	88	66	3
8	PVC	22	110	88	4
9	PVC	22	132	110	5
10	Al (99.95%)	22	44	22	1
11	Al (99.95%)	22	66	44	2
12	Al (99.95%)	22	110	88	4

The critical plastic stress σ_0 operating in PVC when crazing is first observed was determined by evaluating the variation in density with the applied strain during tensile testing (Ref 14). In general terms, the procedure relates the formation of microvoids that gives rise to crazes and to progressive change of color with the variation of density and, in case of the PVC under evaluation, a craze opening stress $\sigma_0 = 50$ MPa was determined.

3.2 Cold Heading

Cylindrical billets of commercial PVC with 22 mm diameter and initial length l_0 in the range 33-132 mm were manufactured from the supplied stock so as to allow the plan of experiments listed in Table 2. The experiments were performed in a simple tool consisting of an upper flat platen and a lower die with a hole (Fig. 1). The tests were carried out in a random order and at least two replicates were produced for each case listed in the table in order to provide statistical meaning.

The experiments were performed with a constant upper flat platen displacement rate of 1.67 mm/s and, under these conditions, no inertial effects on forming mechanisms are likely to occur and, therefore, no dynamic effects in deformation mechanics needed to be taken into account. The tests were carried out under dry friction and these conditions were ensured

by cleaning the tooling with acetone before running each experiment.

The test cases with technically pure aluminum (99.95%) that are included in Table 2 were taken from a previous research work performed by the authors and are mainly utilized for illustrating the differences between cold heading of polymers and metals. Further information on the cold heading of technically pure aluminum can be found elsewhere (Ref 17).

4. Results and Discussion

The experimental work on cold heading of PVC confirmed the existence of three different modes of deformation (Fig. 3). Small values of the slenderness ratio l_u/d_0, which is the ratio of the unsupported length l_u to the diameter d_0 of the billet, allows the material to flow uniformly around its axis of compression and make possible the formation of a sound concentric headed part. On the contrary, large values of the slenderness ratio l_u/d_0 give rise to nonuniform material flow and encourage buckling (bending) at the early stages of deformation. In between these values, failure occurs by material flow resulting from the combination of heading and buckling mechanisms. The experimental observations performed by the authors allowed establishing a threshold value $l_u/d_0 = 1.25$ to produce sound headed PVC parts that is inferior to that of metals (usually in the range up to $l_u/d_0 = 2.5$).

The evolution of the load-displacement curves for cases 3, 6, and 8 of Table 2 is plotted in Fig. 4 and includes several particularities derived from the mechanical behavior of PVC. First, all the curves have a peak of load at the early stages of deformation. Second, the peaks considerably shift to the higher levels of deformation as the slenderness ratio l_u/d_0 of the billets increases. Third, the load-displacement curves at the final stages of deformation exhibit different types of evolutions as a function of the overall feasibility of the cold heading operation.

The first of these particularities is due to the yield strength peaks that are typical of tensile and compressive stress-strain curves of PVC (Fig. 2). Because metals do not show yield strength peaks in the stress-strain curves its load-displacement curves growth monotonically at the beginning of the cold heading process (Fig. 5, refer to Ref 17).

The second type of particularity is also specific from PVC because cold heading of metal billets (e.g., technically pure aluminum in Fig. 5) experiences a steep increase in the compressive load at the early stages of deformation. In fact, one of the characteristics of the cold heading of PVC is that small values of the slenderness ratio l_u/d_0 give rise to a rapid increase of the compressive load, in agreement with what is commonly found in metals, while large values of l_u/d_0 show moderate or low rates of the compressive load from zero up to a maximum value.

Among the factors that contribute toward the aforementioned behavior of the load-displacement curves it is worth noticing the low value of the elasticity modulus of PVC (2.45 GPa) compared with that of metals currently employed in engineering applications (70 GPa in aluminum alloys and 200 GPa in Steels). The low elasticity modulus of PVC gives rise to small critical loads and, therefore, encourages material to flow sideways at the upper unconstrained end of the billets (Fig. 6). This leads to eccentricity of the axial compressive load and to a bending moment acting on the billet.

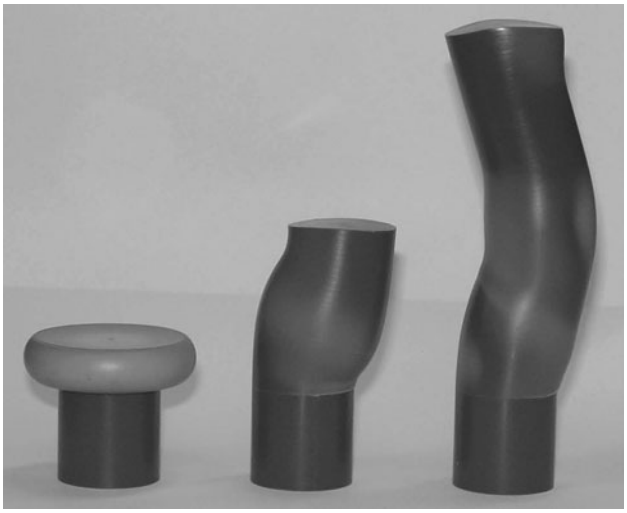

Fig. 3 Typical modes of deformation that occur during cold heading of cylindrical PVC billets (cases 3, 6, and 8 of Table 2)

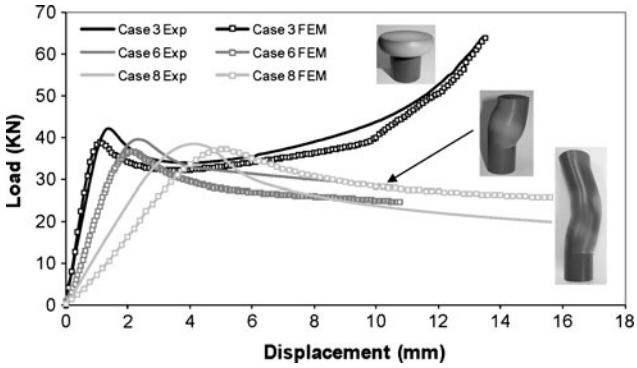

Fig. 4 Theoretical and experimental evolution of the load-displacement curve for the cold heading of cylindrical PVC billets. *Note*: Insets show deformed specimens at the end of the forming process

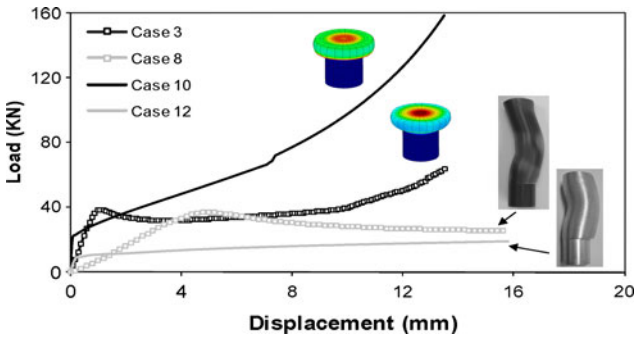

Fig. 5 Theoretical evolution of the load-displacement curve for the cold heading of cylindrical billets made from PVC and technically pure aluminum. *Note*: Insets show computed and experimental specimens at the end of deformation. The computed specimens put into evidence the region where the effective strain rate is higher at the end of the process (around, 0.3 s^{-1})

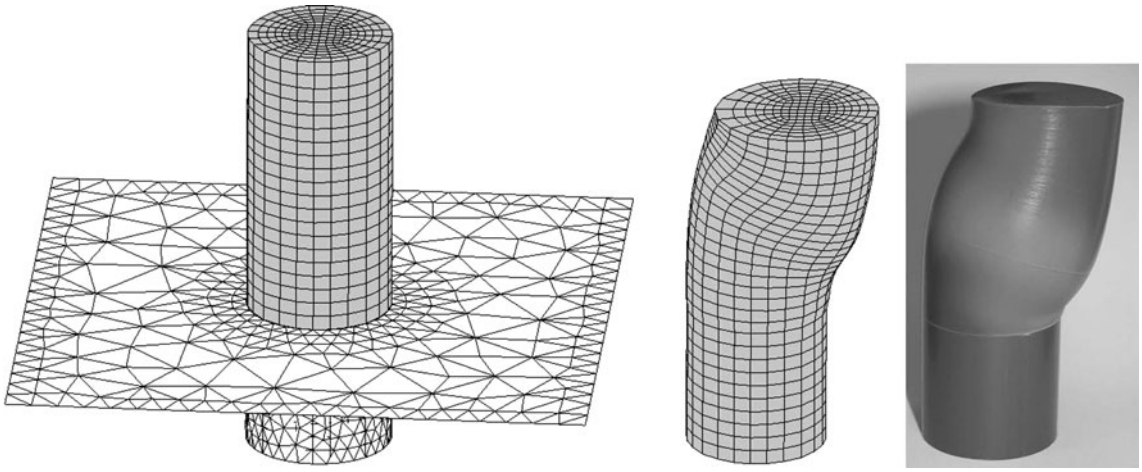

Fig. 6 Initial finite element discretization and comparison between computed and experimental geometry at the end of the cold heading of cylindrical PVC billets (case 6 of Table 2)

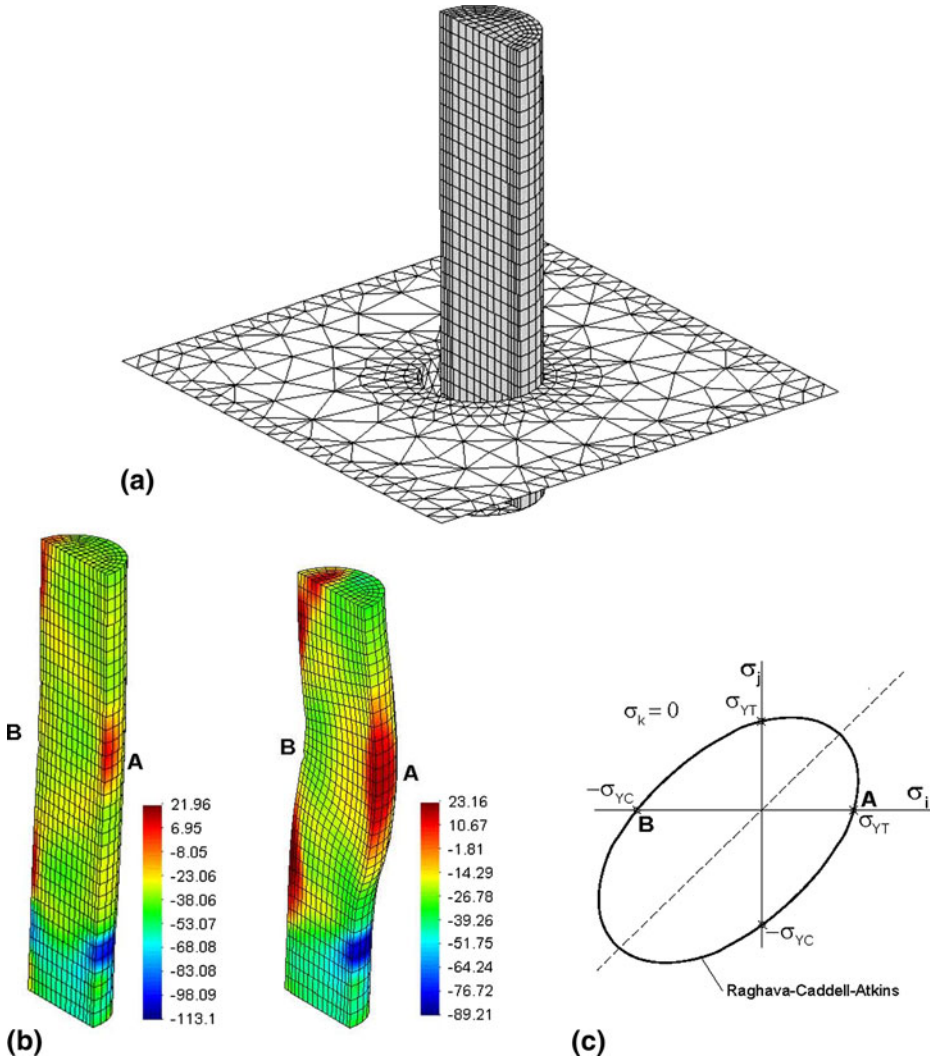

Fig. 7 Computed distribution of the mean stress σ_m (MPa) at the early stages of the cold heading of cylindrical PVC billets (case 8 of Table 2)

In case of slender PVC billets, the portion of the cross section placed on the convex side of the billets experiences near uniaxial tensile loading conditions while the opposite portion, located at the concave (or reentrant) side, is loaded under uniaxial compressive conditions. This explains the distribution of mean stresses σ_m in Fig. 7 and gives support to the

schematic location of regions 'A' and 'B' of the PVC billets in the principal stress space during cold heading (refer to Fig. 7c).

The abovementioned facts, combined with the pressure dependency of the yield function and the strength differential effect of the stress-strain curve of PVC, give rise to an easier plastic flow in the convex side of the billets and to a progressive drift from linearity as the slenderness ratio l_u/d_0 increases. In view of this, the influence of geometrical irregularities of tooling in the overall plastic deformation of PVC billets is more pronounced than in metals.

In what concerns the third type of particularity, Fig. 4 shows that the load-displacement curve at the final stages of deformation can growth from a lowered level as upset takes place (case 3 of Table 2) or continuously diminishing as buckling progresses (cases 6 and 8 of Table 2). The later evolution is because bent forms of equilibrium, resulting from buckling, need small values of the axial compressive load as the degree of bending increases.

The agreement between experimental and finite element estimates of the load-displacement curve (Fig. 4) is very good and confirms the effectiveness of the extended finite element flow formulation to model the cold plastic deformation of polymers. Major differences are found to occur in the vicinity of the peak loads and in replicating the initial loading rate of case 8 (Table 2).

PVC billets also experience a certain amount of crazing during cold heading. Crazes are crack-like defects (but are not true cracks) that are characterized by regions of highly plastically deformed material interspersed with voids (Ref 18) and are expected to be triggered when the normalized ratio of the stress-bias criterion $\sigma_1/\sigma_0 > 1$ (refer to Section 2.2). Figure 8 contains the distribution of the normalized ratio of the stress-bias criterion (Ref 10) for the final deformation stage of case 6 (Table 2). The maximum values are placed at the back side of the specimen, and this explains the reason why the color of this region becomes lighter (due to stress whitening) than the original gray color of the PVC billet at the beginning of the process.

Figure 9 shows the experimental and the finite element predicted cross section of a cold headed PVC billet (case 2 of

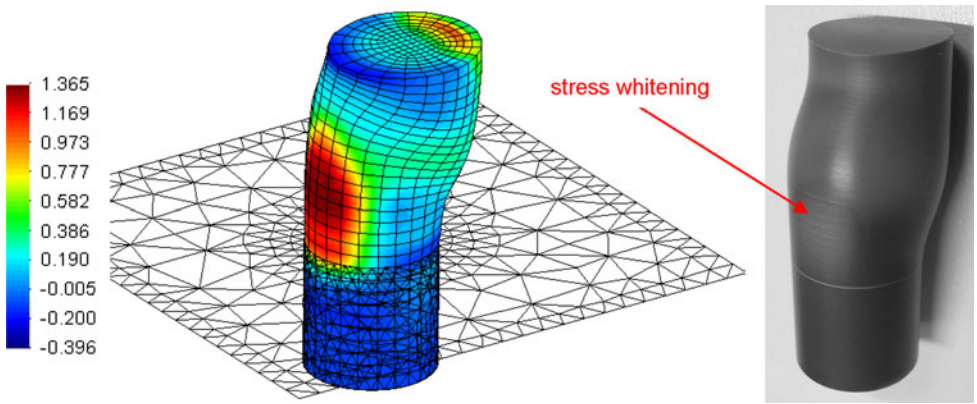

Fig. 8 Cold heading of cylindrical PVC billets (case 6 of Table 2). Theoretical estimate of crazing according to the normalized version of the stress-bias criterion and experimental evidence of "stress whitening"

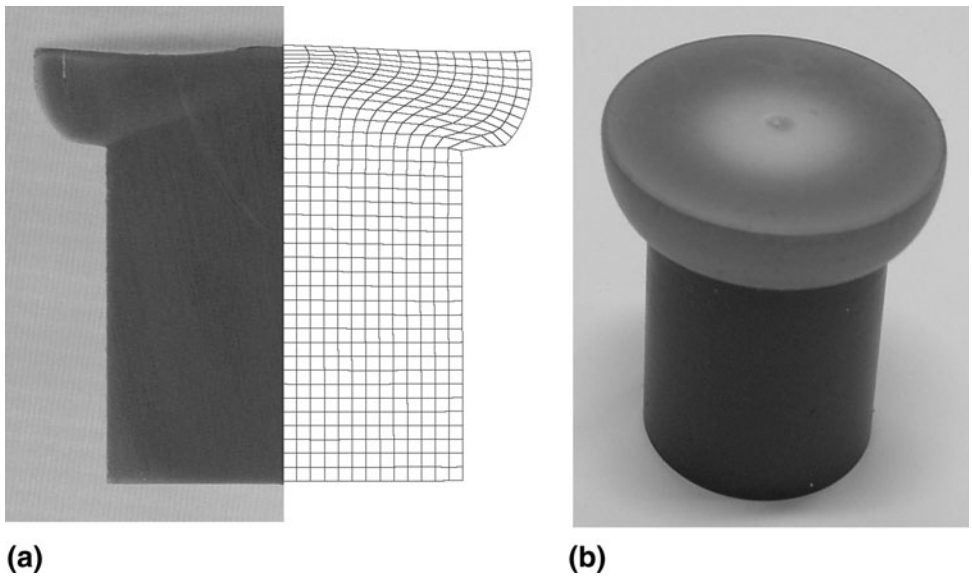

Fig. 9 Elastic recovery of a cold headed PVC part (case 2 of Table 2). (a) Computed and experimental profile of the cross section after unloading and removal of the part from tooling. (b) Detail of the upper end showing stress whitening at the center

Table 2) upon unloading and removal of the part from tooling. The correlation is very good and shows that the upper upset end of the billet is not flat, as in case of metals. In fact, it presents a small depression located in-between the center and the outside diameter, which seems to be a consequence of the accumulation of crazes in that region of the specimen (Fig. 9b).

5. Conclusions

This paper evaluates the possibility of employing cold heading, currently utilized in metals, to the production of upset shapes at the ends of cylindrical PVC billets.

The investigation showed that the formability limits of the process are directly related to the slenderness ratio l_u/d_0 of the unsupported length to the diameter of the billet, as in case of metals. Beyond a critical value of l_u/d_0, which was determined to be roughly equal to half the value commonly utilized in metals, the PVC billets are likely to buckle or bend, forcing material to one side and preventing the formation of a concentric part. However, in case of PVC, the accumulation of crazes also needs to be taken into consideration because it will account for the overall quality and appearance of the upset formed parts and for the final geometry of the part upon unloading and removal from tooling.

The investigation also revealed that the influence of geometrical irregularities of tooling in cold heading of PVC parts is more pronounced than in metals due to particularities of the stress-strain curves of PVC derived from the strength differential effect and the yield strength peaks.

Finally, the overall research work demonstrates that numerical simulation by means of the innovative extension of the flow formulation that is capable of modeling cold plastic deformation of pressure-sensitive polymers under a nonassociated flow rule, allows successful modeling cold heading of cylindrical PVC billets.

Acknowledgment

The authors acknowledge the financial support provided by FCT-Portugal.

References

1. Carpenter Technology Corporation, Cold Heading, *Am. Fasten. J.*, 2004, **21**(2), p 56–58
2. A.G. Lecocq, Stresses in the Shank of a Bolt During Cold Heading, *Wire*, 1971, **115**, p 197
3. S.N. Shah and S. Kobayashi, Rigid-Plastic Analysis of Cold Heading by the Matrix Method, *Proc. 15th. International Machine Tool Design Research Conference*, 1974, p 603–610
4. K. Lange, *Handbook of Metal Forming*, McGraw-Hill, New York, 1985
5. K. Mori, K. Osakada, and S. Kadohata, Finite Element Simulation of Three-Dimensional Buckling in Upsetting and Heading of Cylindrical Billet, *Advanced Technology of Plasticity, Proc. 4th. International Conference on Technology of Plasticity*, 1993, p 1047–1052
6. J. Mackerle, Finite-Element Analysis and Simulation of Polymers: A Bibliography (1976-1996), *Model. Simulat. Mater. Sci. Eng.*, 1997, **5**, p 615–650
7. J. Mackerle, Finite Element Analysis and Simulation of Polymers—An Addendum: A Bibliography (1996-2002), *Model. Simulat. Mater. Sci. Eng.*, 2003, **11**, p 195–231
8. W. Whitney and R.D. Andrews, Yielding of Glassy Polymers: Volume Effects, *J. Polym. Sci. C*, 1967, **16**, p 2981–2990
9. S.S. Sternstein and L. Ongchin, Yield Criteria for Plastic Deformation of Glassy High Polymers in General Stress Fields, *Polym. Preprint Am. Chem. Soc.*, 1969, **10**, p 1117–1124
10. R.S. Raghava, R.M. Caddell, and G.S.Y. Yeh, The Macroscopic Yield Behaviour of Polymers, *J. Mater. Sci.*, 1973, **8**, p 225–232
11. R.M. Caddell, R.S. Raghava, and A.G. Atkins, Pressure Dependent Yield Criteria for Polymers, *Mater. Sci. Eng.*, 1974, **13**, p 113–120
12. W.A. Spitzig and O. Richmond, Effect of Hydrostatic Pressure on the Deformation Behaviour of Polyethylene and Polycarbonate in Tension and in Compression, *Polym. Eng. Sci.*, 1979, **19**, p 1129–1139
13. M.L. Alves, J.M.C. Rodrigues, and P.A.F. Martins, Three-Dimensional Modelling of Forging Processes by the Finite Element Flow Formulation, *J. Eng. Manuf.*, 2004, **218**, p 1695–1708
14. L.M. Alves and P.A.F. Martins, Nosing of Thin-Walled PVC Tubes into Hollow Spheres Using a Die, *Int. J. Adv. Manuf. Technol.*, 2009, **44**, p 26–37
15. J.H. Lee and J. Oung, Yield Functions and Flow Rules for Porous Pressure-Dependent Strain-Hardening Polymeric Materials, *J. Appl. Mech. Trans. ASME*, 2000, **67**, p 288–297
16. C.B. Bucknall, New Criterion for Craze Initiation, *Polymer*, 2007, **48**, p 1030–1041
17. M.L. Alves, J.M.C. Rodrigues, and P.A.F. Martins, Finite Element Modelling of Forging Processes Using the Flow Formulation, *ICIT 2005-V International Conference on Industrial Tools*, Velenje, Slovenia, 2005
18. D.K. Felbeck and A.G. Atkins, *Strength and Fracture of Engineering Solids*, Prentice Hall, NJ, 1996